Supplementary Material

Code for the model, along with simulation movies, can be found at the GitHub repository: `https://github.com/melissahmai/` `threesphere`.

Supplementary Movie Captions

- Movie 1: Anti-parallel cells at low adhesion, corresponding with the parameters of Fig. 6a.

- Movie 2: Anti-parallel cells at high adhesion, corresponding with the parameters of Fig. 6b.

- Movie 3 and 4: Swimmer with four crawlers in the same (3) or opposite (4) direction. Parameters correspond to those of Fig. 7.

Supplementary Figures
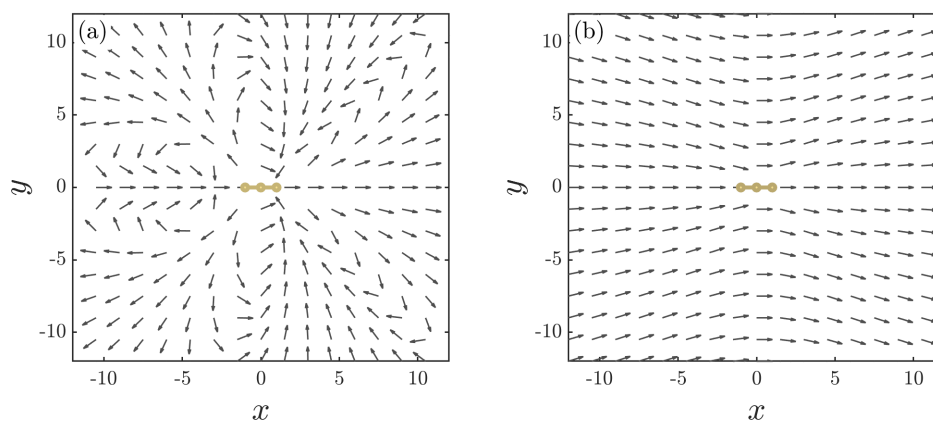
Fig. S1 Far-field time-averaged flow fields for a swimmer ($\xi/6\pi\eta L = 0$) (a) and a crawler ($\xi/6\pi\eta L = 10^3$) (b) moving to the right far from a wall.
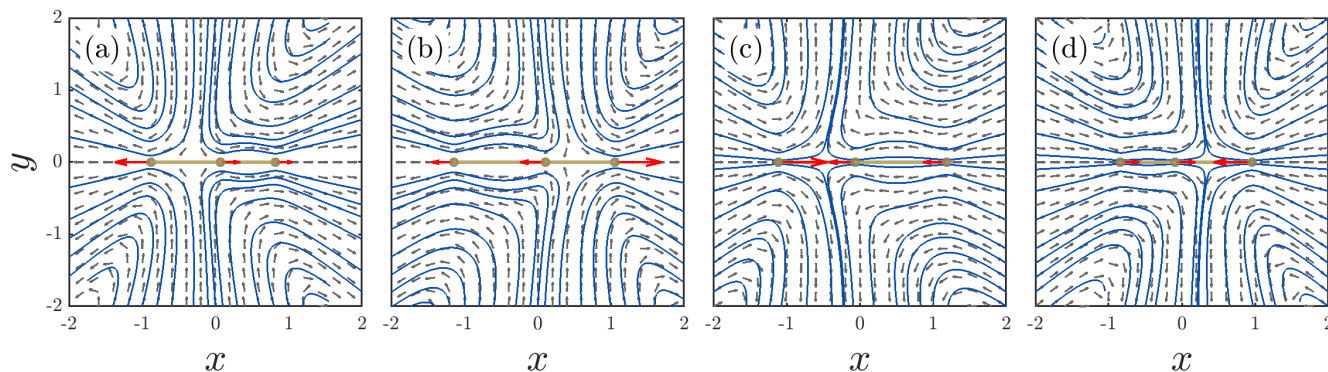
Fig. S2 Instantaneous streamlines (blue) and flow field (gray) around a swimmer ($\xi/6\pi\eta L = 0$) far from a wall through its axis during each phase of motion. The total force on each bead is illustrated by the red arrows. The flow field around each phase resembles that of a positive (a-b) or negative (c-d) force dipole flow, corresponding to extension or contraction of the cell.
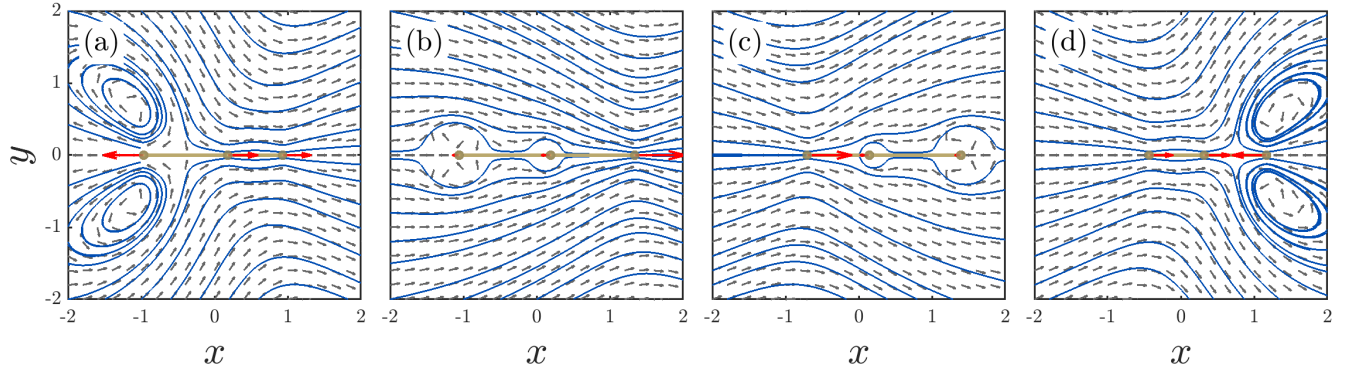
Fig. S3 Instantaneous streamlines (blue) and flow field (gray) around a crawler ($\xi/6\pi\eta L = 10^3$) on a fiber far from a wall through its axis during each phase of motion. The total force on each bead is illustrated by the red arrows. During trailing arm extension (a), the trailing and center bead must both exert a large internal force to overcome strong adhesion, creating a flow field that roughly resembles a positive force dipole. (b-c) During leading arm extension (b) and trailing arm contraction (c), the beads for the trailing and leading arms, respectively, exert little force due to high adhesion and a zero deformation velocity. As a result, the flow field behaves as that of a Stokeslet around the mobile bead. During leading arm contraction (d), since the leading and center beads are moving in spite of strong adhesion, the flow field again roughly resembles a force dipole, though now negative.
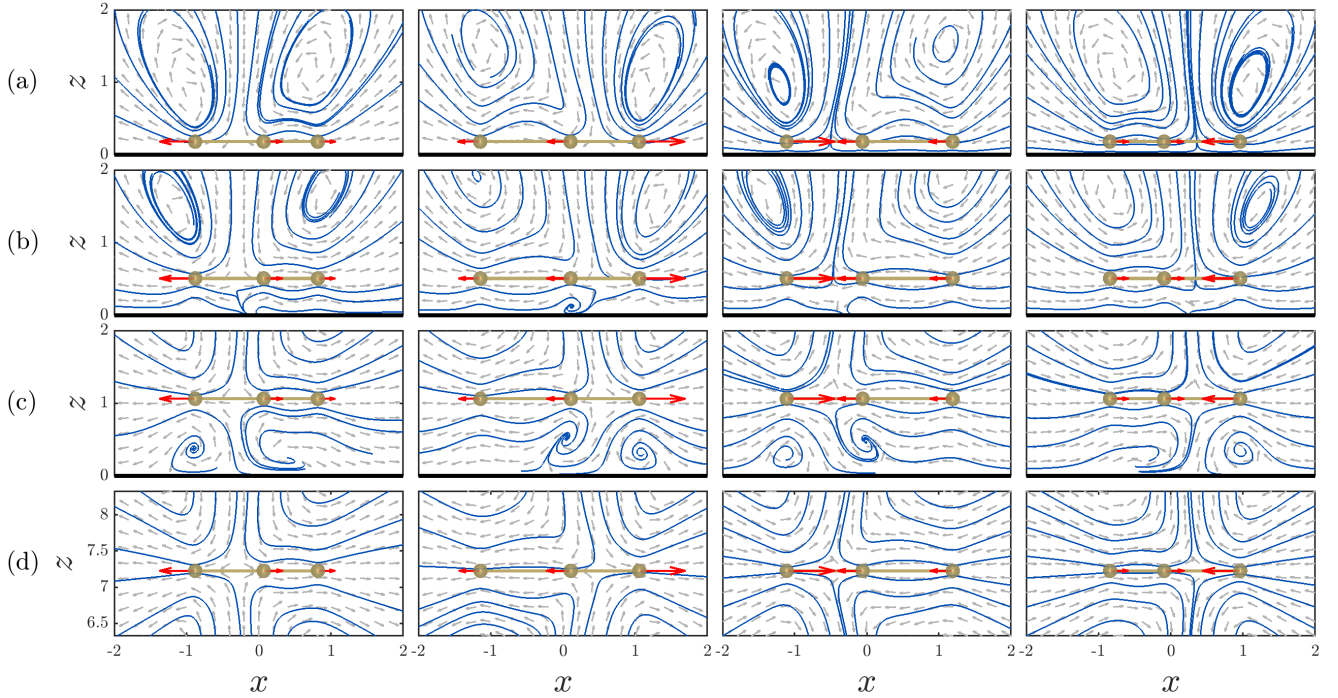
Fig. S4 Instantaneous streamlines (blue) and flow field (gray) around a cell at very low adhesion ($\xi/6\pi\eta L = 10^{-3}$) on a fiber at varying heights during each phase of motion. The total force on each bead is illustrated by the red arrows. The substrate surface at $z = 0$ is shown in the thick black line. (a) $z = 2a$. The cell is just hovering over the surface and is in the first region of increasing velocity in Fig. 4b. (b) $z = 5a$. The cell is high enough off the wall to allow for flow underneath it, but close enough to still be affected by the wall. The cell exists in the intermediate plateau in the velocity profile of Fig. 4b. (c) $z = 10a$. The cell is high enough off the wall to create vortices underneath, and velocity again is increasing. (d) $z > 50a$. The cell is far enough away from the wall to no longer be affected by its hydrodynamics. Note that in these figures, as in Fig. 5 in the main paper, local streamlines can be misleading; no-slip boundary conditions are obeyed at $z = 0$.
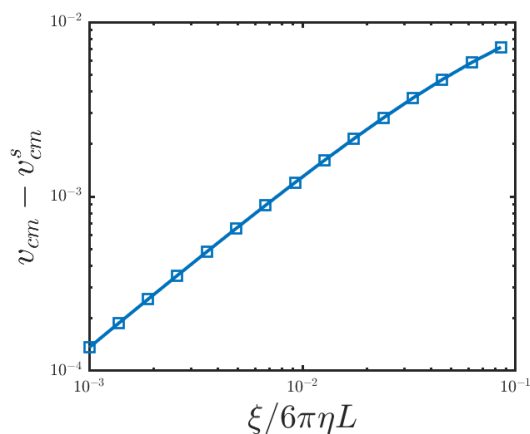
Fig. S5 Log-log representation of the center-of-mass velocity, with the velocity of the swimmer (zero adhesion) subtracted off, in the limit of small $\xi/6\pi\eta L$. The dependence of this increase is roughly linear.
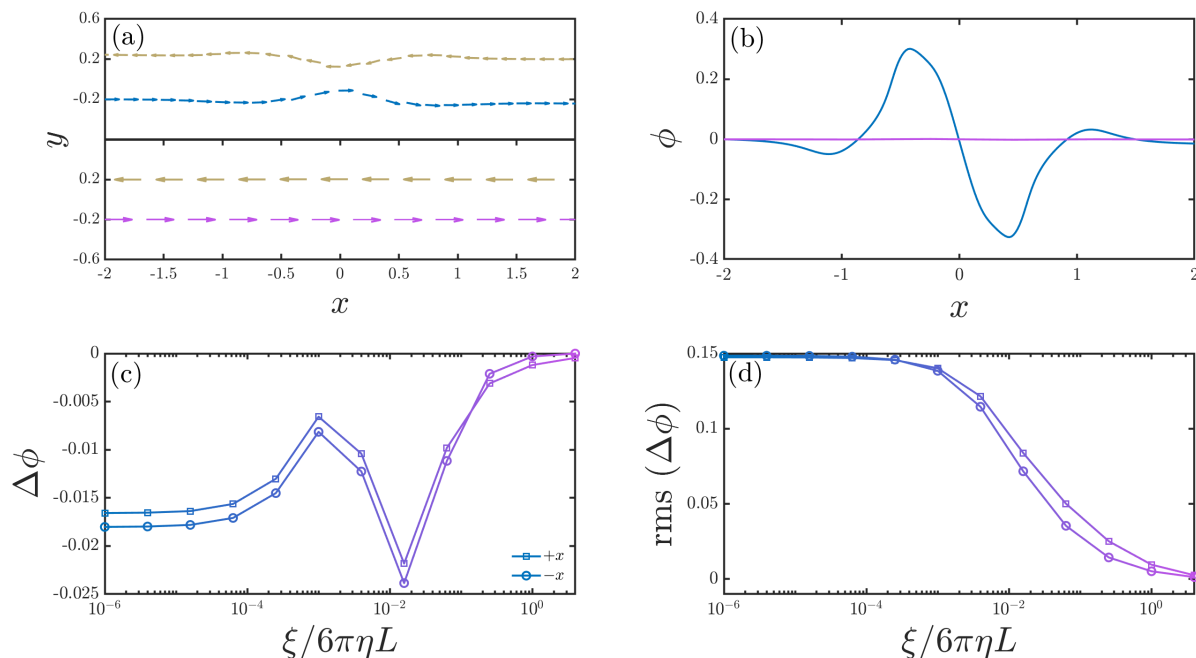
Fig. S6 (a) Trajectories for two antiparallel cells, out of phase by half a motion cycle, at low (blue) and high (purple) adhesion. The $-x$ oriented cell is shown in yellow. (b) Angle ϕ of the $+x$-oriented cell, shown as a function of the cell's center of mass position (large x corresponding to post-interaction). (c) Net angular deflection ($\Delta\phi$) of the $+x$ (square) and $-x$ (circle) oriented cells as a function of $\xi/6\pi\eta L$ is both small and non-monotonic with adhesion strength, suggesting that sometimes another metric must be used to characterize hydrodynamic interactions. (d) RMS deflection, calculated per cycle over the period of interaction, defined as the time over which the cells are within a certain distance of each other (in this case $d = 4L$), exhibits monotonic behavior over $\xi/6\pi\eta L$ and may be a useful metric of hydrodynamic interactions when net deflection is insufficient.

Analytical results in the large-adhesion limit

In the large-adhesion limit, we can neglect hydrodynamics and Eq. 15 is equivalent to:

$$\mathbf{V} = \frac{1}{\boldsymbol{\xi}(t)} \circ \mathbf{F}^{\text{int}}, \tag{S1}$$

i.e. the motion of one bead is only controlled by the force on that bead and the friction coefficient on the bead. This allows us to simply compute the velocity of a single cell in the high-adhesion limit. To do this, we simplify to one dimension, following the approach of[28], and find the internal forces that satisfy

$$V_3 - V_2 = F_3^{\text{int}}/\xi_3 - F_2^{\text{int}}/\xi_2 = W_L \tag{S2}$$

$$V_2 - V_1 = F_2^{\text{int}}/\xi_2 - F_1^{\text{int}}/\xi_1 = W_T \tag{S3}$$

$$F_1^{\text{int}} + F_2^{\text{int}} + F_3^{\text{int}} = 0. \tag{S4}$$

This can be done analytically due to the simplicity of the model, though we do not write it explicitly here. These forces then determine

$$v_{\text{cm}}(t) = \frac{1}{3}(V_1 + V_2 + V_3) = \frac{-2W_L\mu_1\mu_2 + 2W_T\mu_2\mu_3 + W_L(\mu_1 + \mu_2)\mu_3 - W_T\mu_1(\mu_2 + \mu_3)}{3\mu_2\mu_3 + 3\mu_1(\mu_2 + \mu_3)} \tag{S5}$$

where $\mu_i = 1/\xi_i$ is a mobility for bead i. This gives the center-of-mass velocity at a given instant, and depends on W_L and W_T as well as $\xi_i(t)$ for each bead. In addition, the forces determine the maximum required force $\max|\mathbf{F}^{\text{req}}|$; we scale the internal forces as in the main text if $\max|\mathbf{F}^{\text{req}}|$ exceeds F^{thresh}.

We can then compute the time average of $v_{\text{cm}}(t)$ over one whole cycle. During each phase of the cycle, the center of mass velocity is constant, so this time average is merely

$$v_{\text{cm}} = \frac{1}{T_{\text{trail-ext}} + T_{\text{lead-ext}} + T_{\text{trail-cont}} + T_{\text{lead-cont}}} \times \tag{S6}$$

$$[T_{\text{trail-ext}}v_{cm}^{\text{trail-ext}} + T_{\text{lead-ext}}v_{cm}^{\text{lead-ext}} + T_{\text{trail-cont}}v_{cm}^{\text{trail-cont}} + T_{\text{lead-cont}}v_{cm}^{\text{lead-cont}}]$$

where the velocities for each phase are worked out by choosing the appropriate values of ξ_1, ξ_2, and ξ_3 and W_L and W_T from Table 1. Note that for working out the time T of each phase, if the arm is contracting with a constant rate W, this time is merely $\Delta L/W$; however, if the force is above the threshold, then the contraction will be slower, taking a time $\frac{\Delta L}{W} \times \frac{\max|\mathbf{F}^{\text{req}}|}{F^{\text{thresh}}}$. Computing the average, and simplifying, yields Eq. 28 in the main text. We have found computer algebra systems (*Mathematica*) useful for keeping track of the special cases for when the force exceeds the threshold.

We find that this analytic result captures our full simulations very well in the large-adhesion limit (Fig. S7).
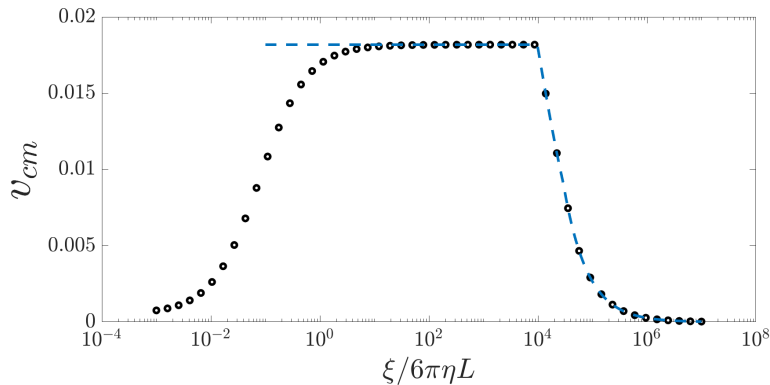
Fig. S7 Comparison between full simulation and the high-friction asymptotic result of Eq. 28. $F^{\text{thresh}} = 10^4$; all other parameters are as in Table S1.

The regularized Blake tensor

We apply the results of[52] to compute how the fluid velocity at point $\mathbf{R}_m$ depends on a force $\mathbf{F}_n$ exerted at point $\mathbf{R}_n$, in the presence of a substrate with a no-slip boundary condition at $z = 0$ (with a normal vector of $\hat{e}_z$). This regularized Green's function generalizes the

simple expressions given in the main paper (Eq. 4 and Eq. 7). The result of[52] is:

$$\mathbf{V}(\mathbf{R}_m, \mathbf{R}_n) = [\mathbf{F}_n H_1(r_n^*) + (\mathbf{F}_n \cdot \mathbf{r}_n^*)\mathbf{r}_n^* H_2(r_n^*)]$$

$$- [\mathbf{F}_n H_1(r_n) + (\mathbf{F}_n \cdot \mathbf{r}_n)\mathbf{r}_n H_2(r_n)]$$

$$- h_n^2 [\mathbf{g}_n D_1(r_n) + (\mathbf{g}_n \cdot \mathbf{r}_n)\mathbf{r}_n D_2(r_n)]$$

$$+ 2h_n \left[\frac{H_1'(r_n)}{r_n} + H_2(r_n) \right] [(\mathbf{F}_n \times \hat{e}_z) \times \mathbf{r}_n]$$

$$+ 2h_n \left[(\mathbf{r}_n g_{nz} + \mathbf{g}_n z_n) H_2(r_n) + (\mathbf{g}_n \cdot \mathbf{r}_n) \left(\hat{e}_z \frac{H_1'(r_n)}{r_n} + \mathbf{r}_n z_n \frac{H_2'(r_n)}{r_n} \right) \right] \quad \text{(S7)}$$

We have defined two relative distances: first, the explicit distance coordinate between the two points, $\mathbf{r}_n^* = \mathbf{R}_m - \mathbf{R}_n$, and the image distance coordinate between the target sphere and the image of the force-generating sphere, $\mathbf{r}_n = \mathbf{R}_m - \mathbf{R}_n + 2h_n\hat{e}_z$. Here, h is the distance of a sphere from the surface, $\mathbf{g}_n = 2(\mathbf{F}_n \cdot \hat{e}_z)\hat{e}_z - \mathbf{F}_n = (-F_{nx}, -F_{ny}, F_{nz})^T$ and z_n is the z-component of $\mathbf{r}_n$. Note that z_n refers to the relative coordinate $\mathbf{r}_n$ and is not equivalent to h_n, which is the z-component of the absolute coordinate $\mathbf{R}_n$. The full derivation for Eq. S7 is available in Reference[52], but we note that the expression above corrects a sign error in its fourth bracketed term, which refers to the image rotlets.

Eq. S7 is still well-defined when $R_m = R_n$. The forces are smoothed over the sphere volumes using four scalar regularization, or "blob," functions:

$$H_1(r) = \frac{1}{8\pi(r^2 + \varepsilon^2)^{1/2}} + \frac{\varepsilon^2}{8\pi(r^2 + \varepsilon^2)^{3/2}} \quad \text{(S8)}$$

$$H_2(r) = \frac{1}{8\pi(r^2 + \varepsilon^2)^{3/2}} \quad \text{(S9)}$$

$$D_1(r) = \frac{1}{4\pi(r^2 + \varepsilon^2)^{3/2}} - \frac{3\varepsilon^2}{4\pi(r^2 + \varepsilon^2)^{5/2}} \quad \text{(S10)}$$

$$D_2(r) = -\frac{3}{4\pi(r^2 + \varepsilon^2)^{5/2}} \quad \text{(S11)}$$

Here ε defines the width of these functions and, therefore, the characteristic length over which to smooth the forces. Thus we set ε equal to the sphere radius a so that the sphere becomes a ball of finite force density instead of a singular point force.

The form Eq. S7 is useful only if the forces on each sphere are already known. Since we must also calculate the individual forces in addition to the velocities through Eq. 10, the expression in Eq. S7 can be rearranged into a more functional form, which is a 3×3 mobility submatrix defined by the hydrodynamic interaction from sphere n acting on sphere m, $\hat{s}_{n \to m}$, that satisfies the relationship defined in Eq. 7. We define the mobility submatrices:

$$\eta \hat{s}_{n \to m} = 2H_2(r) \begin{pmatrix} -2hz & 0 & x(h-z) \\ 0 & 0 & y(h-z) \\ hx & hy & z(2h-z) \end{pmatrix} + H_2(r^*) \begin{pmatrix} x^{*2} & x^*y^* & x^*z^* \\ x^*y^* & y^{*2} & y^*z^* \\ x^*z^* & y^*z^* & z^{*2} \end{pmatrix}$$

$$+ \left[h^2 D_2(r) - H_2(r) - 2h\left(\frac{H_2'(r)}{r} \right) z \right] \begin{pmatrix} x^2 & xy & -xz \\ xy & y^2 & -yz \\ xz & yz & -z^2 \end{pmatrix}$$

$$+ h^2 D_1(r) \begin{pmatrix} 1 & 0 & 0 \\ 0 & 1 & 0 \\ 0 & 0 & -1 \end{pmatrix} + 2h\left(\frac{H_1'(r)}{r} \right) z \begin{pmatrix} -1 & 0 & 0 \\ 0 & 1 & 0 \\ 0 & 0 & 1 \end{pmatrix}$$

$$+ (H_1(r^*) - H_1(r))\mathbb{I} \quad \text{(S12)}$$

in which the subscripted n is implied on all relevant terms. The standard mobility matrix, $\hat{M}$, is then an arrangement of these mobility

submatrices:

$$\hat{M} = \begin{pmatrix} \hat{s}_{1\to1} & \cdots & \hat{s}_{N\to1} \\ \vdots & \ddots & \vdots \\ \hat{s}_{1\to N} & \cdots & \hat{s}_{N\to N} \end{pmatrix} \tag{S13}$$

To solve the system with friction given by Eq. 15, the modified mobility matrix, $\mathcal{M}$, is numerically calculated. The submatrices, $\mathcal{S}$, are then defined such that

$$\left(\mathbb{1}+\hat{\Xi}\right)^{-1}\hat{M} = \mathcal{M} = \begin{pmatrix} \hat{\mathcal{S}}_{1\to1} & \cdots & \hat{\mathcal{S}}_{N\to1} \\ \vdots & \ddots & \vdots \\ \hat{\mathcal{S}}_{1\to N} & \cdots & \hat{\mathcal{S}}_{N\to N} \end{pmatrix}. \tag{S14}$$

which can now be used for all calculations. For example, to rewrite the constraints presented in Eq. 21-24,

$$W_L = \left[\sum_n \left(\hat{\mathcal{S}}_{n\to3} - \hat{\mathcal{S}}_{n\to2}\right)\mathbf{F}_n\right]\cdot\hat{\alpha} \tag{S15}$$

$$W_T = \left[\sum_n \left(\hat{\mathcal{S}}_{n\to2} - \hat{\mathcal{S}}_{n\to1}\right)\mathbf{F}_n\right]\cdot\hat{\alpha} \tag{S16}$$

$$0 = \left\{\sum_n \left[L_T\left(\hat{\mathcal{S}}_{n\to3} - \hat{\mathcal{S}}_{n\to2}\right) - L_L\left(\hat{\mathcal{S}}_{n\to2} - \hat{\mathcal{S}}_{n\to1}\right)\right]\mathbf{F}_n\right\}\cdot\hat{\beta} \tag{S17}$$

$$0 = \left\{\sum_n \left[L_T\left(\hat{\mathcal{S}}_{n\to3} - \hat{\mathcal{S}}_{n\to2}\right) - L_L\left(\hat{\mathcal{S}}_{n\to2} - \hat{\mathcal{S}}_{n\to1}\right)\right]\mathbf{F}_n\right\}\cdot\hat{\gamma} \tag{S18}$$

Constraint matrices

The constraint matrices are explicitly defined here, using the same notation as before, and where $\delta L = L_T - L_L$.

$$\hat{C}_{swim}\mathbf{d}_{swim} =$$

$$
\left(
\begin{array}{ccccccccc}
1 & 0 & 0 & 1 & 0 & 0 & 1 & 0 & 0 \\
0 & 1 & 0 & 0 & 1 & 0 & 0 & 1 & 0 \\
0 & 0 & 1 & 0 & 0 & 1 & 0 & 0 & 1 \\
\mathscr{T}_{Li1}\beta_i & \mathscr{T}_{Li2}\beta_i & \mathscr{T}_{Li3}\beta_i & 0 & 0 & 0 & \mathscr{T}_{Ti1}\beta_i & \mathscr{T}_{Ti2}\beta_i & \mathscr{T}_{Ti3}\beta_i \\
\mathscr{T}_{Li1}\gamma_i & \mathscr{T}_{Li2}\gamma_i & \mathscr{T}_{Li3}\gamma_i & 0 & 0 & 0 & \mathscr{T}_{Ti1}\gamma_i & \mathscr{T}_{Ti2}\gamma_i & \mathscr{T}_{Ti3}\gamma_i \\
\left(\hat{\mathscr{S}}_{1\to3}-\hat{\mathscr{S}}_{1\to2}\right)\cdot\hat{\alpha} & & & \left(\hat{\mathscr{S}}_{2\to3}-\hat{\mathscr{S}}_{2\to2}\right)\cdot\hat{\alpha} & & & \left(\hat{\mathscr{S}}_{3\to3}-\hat{\mathscr{S}}_{3\to2}\right)\cdot\hat{\alpha} & & \\
\left(\hat{\mathscr{S}}_{1\to2}-\hat{\mathscr{S}}_{1\to1}\right)\cdot\hat{\alpha} & & & \left(\hat{\mathscr{S}}_{2\to2}-\hat{\mathscr{S}}_{2\to1}\right)\cdot\hat{\alpha} & & & \left(\hat{\mathscr{S}}_{3\to2}-\hat{\mathscr{S}}_{3\to1}\right)\cdot\hat{\alpha} & & \\
\left[L_T\hat{\mathscr{S}}_{1\to3}+L_L\hat{\mathscr{S}}_{1\to1}-\delta L\hat{\mathscr{S}}_{1\to2}\right]\cdot\hat{\beta} & & & \left[L_T\hat{\mathscr{S}}_{2\to3}+L_L\hat{\mathscr{S}}_{2\to1}-\delta L\hat{\mathscr{S}}_{2\to2}\right]\cdot\hat{\beta} & & & \left[L_T\hat{\mathscr{S}}_{3\to3}+L_L\hat{\mathscr{S}}_{3\to1}-\delta L\hat{\mathscr{S}}_{3\to2}\right]\cdot\hat{\beta} & & \\
\left[L_T\hat{\mathscr{S}}_{1\to3}+L_L\hat{\mathscr{S}}_{1\to1}-\delta L\hat{\mathscr{S}}_{1\to2}\right]\cdot\hat{\gamma} & & & \left[L_T\hat{\mathscr{S}}_{2\to3}+L_L\hat{\mathscr{S}}_{2\to1}-\delta L\hat{\mathscr{S}}_{2\to2}\right]\cdot\hat{\gamma} & & & \left[L_T\hat{\mathscr{S}}_{3\to3}+L_L\hat{\mathscr{S}}_{3\to1}-\delta L\hat{\mathscr{S}}_{3\to2}\right]\cdot\hat{\gamma} & &
\end{array}
\right)
\begin{pmatrix}0\\0\\0\\0\\0\\W_L\\W_T\\0\\0\end{pmatrix}
\begin{matrix}i\\ii\\iii\\iv\\v\\vi\\vii\\viii\\ix\end{matrix}
\qquad (S19)
$$

$$\hat{C}_{crawl}\mathbf{d}_{crawl} =$$

$$
\left(
\begin{array}{ccccccccc}
1 & 0 & 0 & 1 & 0 & 0 & 1 & 0 & 0 \\
0 & 1 & 0 & 0 & 1 & 0 & 0 & 1 & 0 \\
\mathscr{T}_{Li1}\beta_i & \mathscr{T}_{Li2}\beta_i & \mathscr{T}_{Li3}\beta_i & 0 & 0 & 0 & \mathscr{T}_{Ti1}\beta_i & \mathscr{T}_{Ti2}\beta_i & \mathscr{T}_{Ti3}\beta_i \\
\left(\hat{\mathscr{S}}_{1\to3}-\hat{\mathscr{S}}_{1\to2}\right)\cdot\hat{\alpha} & & & \left(\hat{\mathscr{S}}_{2\to3}-\hat{\mathscr{S}}_{2\to2}\right)\cdot\hat{\alpha} & & & \left(\hat{\mathscr{S}}_{3\to3}-\hat{\mathscr{S}}_{3\to2}\right)\cdot\hat{\alpha} & & \\
\left(\hat{\mathscr{S}}_{1\to2}-\hat{\mathscr{S}}_{1\to1}\right)\cdot\hat{\alpha} & & & \left(\hat{\mathscr{S}}_{2\to2}-\hat{\mathscr{S}}_{2\to1}\right)\cdot\hat{\alpha} & & & \left(\hat{\mathscr{S}}_{3\to2}-\hat{\mathscr{S}}_{3\to1}\right)\cdot\hat{\alpha} & & \\
\left[L_T\hat{\mathscr{S}}_{1\to3}+L_L\hat{\mathscr{S}}_{1\to1}-\delta L\hat{\mathscr{S}}_{1\to2}\right]\cdot\hat{\gamma} & & & \left[L_T\hat{\mathscr{S}}_{2\to3}+L_L\hat{\mathscr{S}}_{2\to1}-\delta L\hat{\mathscr{S}}_{2\to2}\right]\cdot\hat{\gamma} & & & \left[L_T\hat{\mathscr{S}}_{3\to3}+L_L\hat{\mathscr{S}}_{3\to1}-\delta L\hat{\mathscr{S}}_{3\to2}\right]\cdot\hat{\gamma} & & \\
\hat{\mathscr{S}}_{1\to1}\cdot\hat{e}_z & & & \hat{\mathscr{S}}_{2\to1}\cdot\hat{e}_z & & & \hat{\mathscr{S}}_{3\to1}\cdot\hat{e}_z & & \\
\hat{\mathscr{S}}_{1\to2}\cdot\hat{e}_z & & & \hat{\mathscr{S}}_{2\to2}\cdot\hat{e}_z & & & \hat{\mathscr{S}}_{3\to2}\cdot\hat{e}_z & & \\
\hat{\mathscr{S}}_{1\to3}\cdot\hat{e}_z & & & \hat{\mathscr{S}}_{2\to3}\cdot\hat{e}_z & & & \hat{\mathscr{S}}_{3\to3}\cdot\hat{e}_z & &
\end{array}
\right)
\begin{pmatrix}0\\0\\0\\W_L\\W_T\\0\\0\\0\\0\end{pmatrix}
\begin{matrix}i\\ii\\iii\\iv\\v\\vi\\vii\\viii\\ix\end{matrix}
\qquad (S20)
$$

When we define the constraints that keep the cell torque-free, we use

$$\hat{\mathcal{T}}_L = \begin{pmatrix} 0 & z_L & -y_L \\ -z_L & 0 & x_L \\ y_L & -x_L & 0 \end{pmatrix} \qquad\qquad \hat{\mathcal{T}}_T = \begin{pmatrix} 0 & z_T & -y_T \\ -z_T & 0 & x_T \\ y_T & -x_T & 0 \end{pmatrix}$$

where x_L indicates the displacement of the leading arm in the x direction, etc.

The rows of each constraint matrix correspond to the following constraints:

For swimming (Eq. S19),

i-iii: Force-free conditions

iv-v: Torque-free conditions (projection onto $\hat{\beta}$ and $\hat{\gamma}$)

vi: Leading arm deformation velocity

vii: Trailing arm deformation velocity

viii-ix: Rigid body conditions with projections of the deformation velocities onto $\hat{\beta}$ and $\hat{\gamma}$, respectively

For crawling (Eq. S20),

i-ii: Force-free conditions

iii: z-component ($\hat{\beta}$-projection) of the torque-free condition

iv: Leading arm deformation velocity

v: Trailing arm deformation velocity

vi: Rigid body condition with projection of the deformation velocities onto $\hat{\gamma}$

vii-ix: Zero z-directional velocities for each sphere

Parameters

Below are the parameters used for the simulations discussed in this project. Parameters are given in the simulation units discussed in the Methods of the main paper. Table S1 provides all the parameters for the standard simulation. Tables S2-S3 refer to their respective simulations discussed above. Parameters not listed in Tables S2-S3 are unchanged from the standard parameter values given in Table S1.

Table S1 Parameters for the standard simulation

Parameter	Symbol	Value
Mean arm length	L	1
Bead radius	a	0.1
Initial center of mass	$\mathbf{R}_{com}(t=0)$	$(0,0,a)$
Deformation magnitude	ΔL	± 0.5
Deformation velocities	$W_L^+, W_L^-, W_T^+, W_T^-$	± 0.1
Polar angle	θ	$\pi/2$
Azimuthal angle	ϕ	0
High adhesion scale	ξ_{high}	ξ
Low adhesion scale	ξ_{low}	0.2ξ
Viscosity	η	1
Threshold force	F^{thresh}	10^3
Time step	Δt	10^{-2}

Table S2 Parameters for the anti-aligned pair

Parameter	Cell 1	Cell 2
Initial center of mass, $\mathbf{R}_{com}(t=0)$	(-2, -0.2, 0.1)	(2, 0.2, 0.1)
Azimuthal Angle, ϕ	0	π
Global adhesion (swim), ξ	$10^{-6} \cdot 6\pi$	
Global adhesion (crawl), ξ	$10^3 \cdot 6\pi$	

Table S3 Parameters for the swimmer among multiple crawlers. Crawlers are generated every 90 cycles and removed from the system once the distance between the swimmer and crawler is sufficiently large (after around 60 cycles) to reduce computational load. $\mathbf{R}_{com}^{c,\pm x}(t_{gen})$ refers to the center of mass of each crawler at the time of its generation.

Parameter	Value
$\mathbf{R}_{com}^s(t=0)$	(0, 0, 1)
Time between crawlers	90 cycles
$\mathbf{R}_{com}^{c,+x}(t_{gen})$	(-3, 0, 0.1)
$\mathbf{R}_{com}^{c,-x}(t_{gen})$	(8, 0, 0.1)
Crawler deformation velocity, W_c	± 0.05
Crawler deformation magnitude ΔL_c	± 0.25
Azimuthal Angle, ϕ	0 or π
Global adhesion (swim), ξ	0
Global adhesion (crawl), ξ	$10^4 \cdot 30\pi$
F^{thresh}	10^5